

## Supporting Information for

# Nitrogen doped CoP on Ammoniated Black Phosphorus Nanosheets Enabling Highly Efficient Hydrogen Evolution Electrocatalysis

Liang Fang<sup>a,\*</sup>, Yanping Xie<sup>b</sup>, Feiya Xu<sup>b</sup>, Miao Wang<sup>c</sup> and Gang Wang<sup>a</sup>

*a. Collaborative Innovation Center of Henan Province for Energy-Saving Building Materials Xinyang Normal University, Xinyang, Henan, 464000, P.R. China*

*b. Analysis & Testing Center, Xinyang Normal University, Xinyang, Henan, 464000, China*

*c. College of Chemistry and Chemical Engineering, Xinyang Normal University, Xinyang 464000, China*

*\*Corresponding author. Tel: +86-376-6370838.*

*E-mail address: fangliang@xynu.edu.cn (L. Fang)*

## Table of contents

**Figure S1.** HRTEM image of BP nanosheets.

**Figure S2.** SEM image of CoP@BP.

**Figure S3.** SEM images of BP nanosheets (a) and BP nanosheets well-adsorbed with Co ions (b).

**Figure S4.** EDS analysis of N-CoP/NH<sub>2</sub>-BP.

**Figure S5.** FTIR spectra of N-CoP/NH<sub>2</sub>-BP.

**Figure S6.** Overpotentials comparison between N-CoP/NH<sub>2</sub>-BP and CoP/BP at different current densities.

---

\* Corresponding author. Tel: +86-376-6370838. E-mail address: fangliang@xynu.edu.cn (L. Fang)

**Table S1.** HER performances of previously reported non-noble electrocatalysts in alkaline electrolyte.

**Figure S7.** CV curves of BP/CoP and N-CoP/NH<sub>2</sub>-BP at different scans.

**Figure S8.** Polarization curves with current density normalized by ECSA for N-CoP/NH<sub>2</sub>-BP and CoP/BP.

**Note S1.** Turn over frequency (TOF) of N-CoP/NH<sub>2</sub>-BP and CoP/BP catalysts.

**Table S2.** Fitting results of the EIS curves in Fig.5e using the equivalent circuit.

**Figure S9.** HRTEM image of N-CoP/NH<sub>2</sub>-BP after i-t test.

**Figure S10.** The element mapping images of N-CoP/NH<sub>2</sub>-BP after HER test

**Figure S11.** (a) XPS survey, high-resolution XPS spectra of (b) Co 2p, (c) P 2p, and (d) N 1s of the N-CoP/NH<sub>2</sub>-BP electrode before and after stability test.

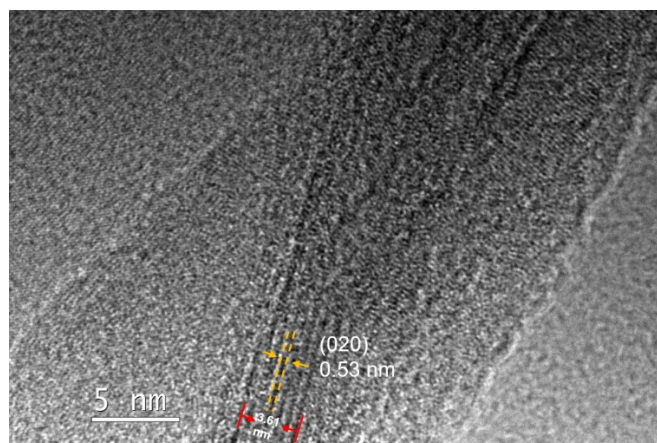


**Figure S1.** HRTEM image of BP nanosheets.

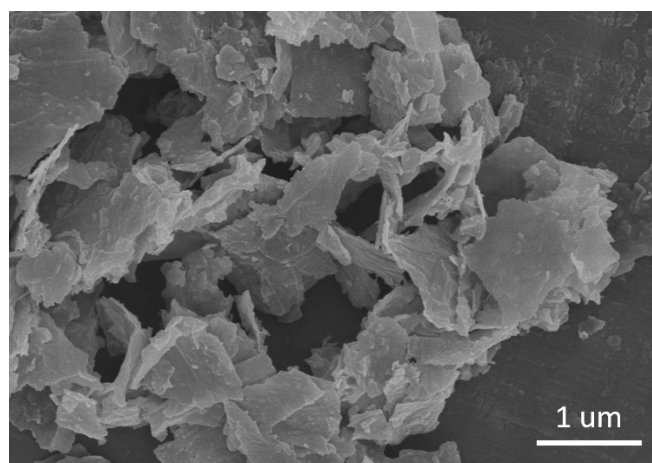


**Figure S2.** SEM image of CoP@BP.

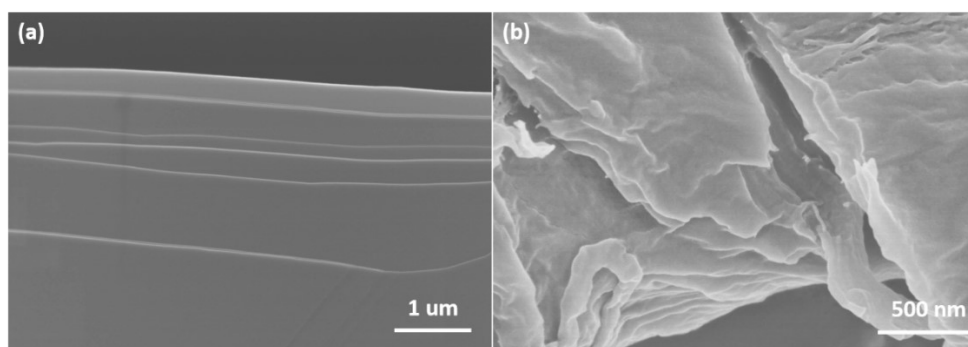


**Figure S3.** SEM images of BP nanosheets (a) and BP nanosheets well-adsorbed with Co ions (b).

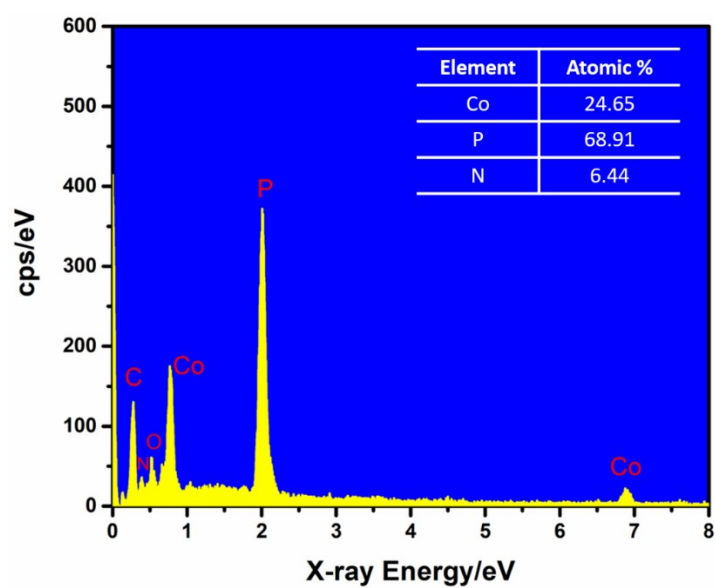


**Figure S4.** EDS analysis of N-CoP/NH<sub>2</sub>-BP.

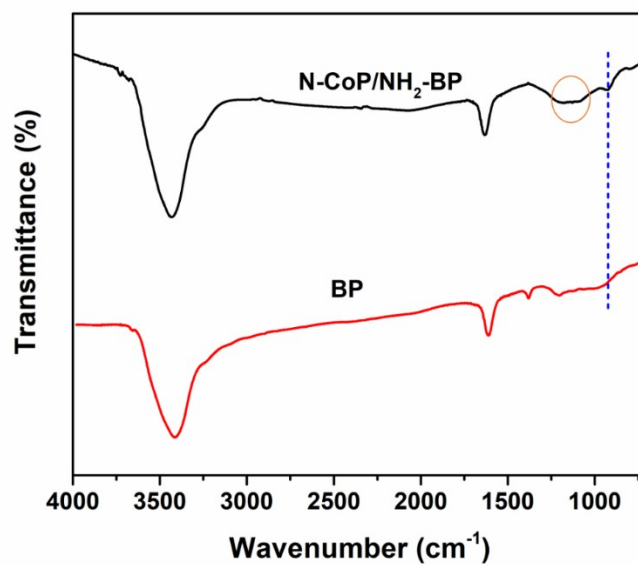


**Figure S5.** FTIR spectra of N-CoP/NH<sub>2</sub>-BP. Relative to BP, a wide weak absorption peak at 1100~1200 cm<sup>-1</sup> in N-CoP/NH<sub>2</sub>-BP was found, which should be attributed to the rock vibration of NH<sub>2</sub>. The identifiable absorption peaks are weak, due to the surface oxidation of nanosheets in air.

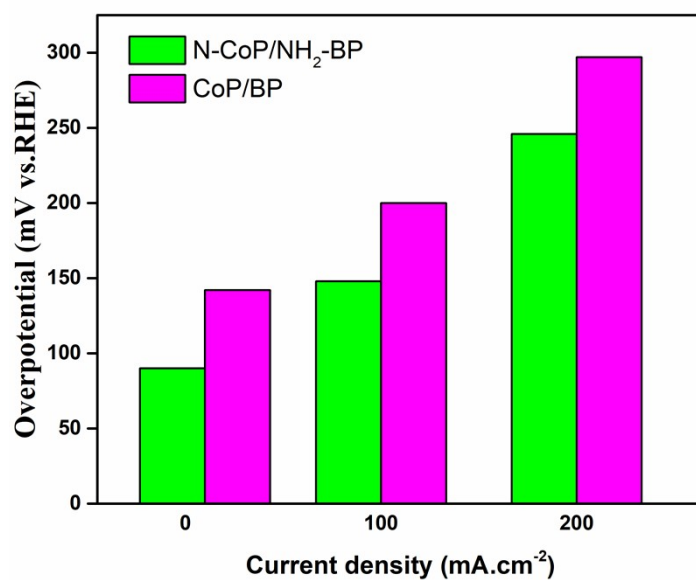


**Figure S6.** Overpotentials comparison between N-CoP/NH<sub>2</sub>-BP and CoP/BP at different current densities.

**Table S1.** HER performances of previously reported non-noble electrocatalysts in alkaline electrolyte.

Catalysts	$\eta$ (mV)	Current density $\text{mA cm}^{-2}$	Tafel slopes $\text{mV dec}^{-1}$	Electrolyte	Ref.
N-CoP/NH <sub>2</sub> -BP	90	10	52.2	1M KOH	This work
	246	200			
BPed-Pt/GR	21	10	46.9	1M KOH	(1)
BP/Co <sub>2</sub> P	336	100	72	1M KOH	(2)
BP QDs/MXene	190	10	83	1M KOH	(3)
NH <sub>2</sub> -BP	290	10	67	1M KOH	(4)
PtRu NCs/BP	22	10	19	1M KOH	(5)
MoS <sub>2</sub> /BP	85	10	68	0.5 M H <sub>2</sub> SO <sub>4</sub>	(6)
Ni <sub>2</sub> P/BP	107	10	38.6	0.5 M H <sub>2</sub> SO <sub>4</sub>	(7)
BP particles	880	10		0.5 M H <sub>2</sub> SO <sub>4</sub>	(8)
CC@N-CoP	42	10	41.2	0.5 M H <sub>2</sub> SO <sub>4</sub>	(9)
CoP nanosheets	131	100	44	0.5 M H <sub>2</sub> SO <sub>4</sub>	(10)

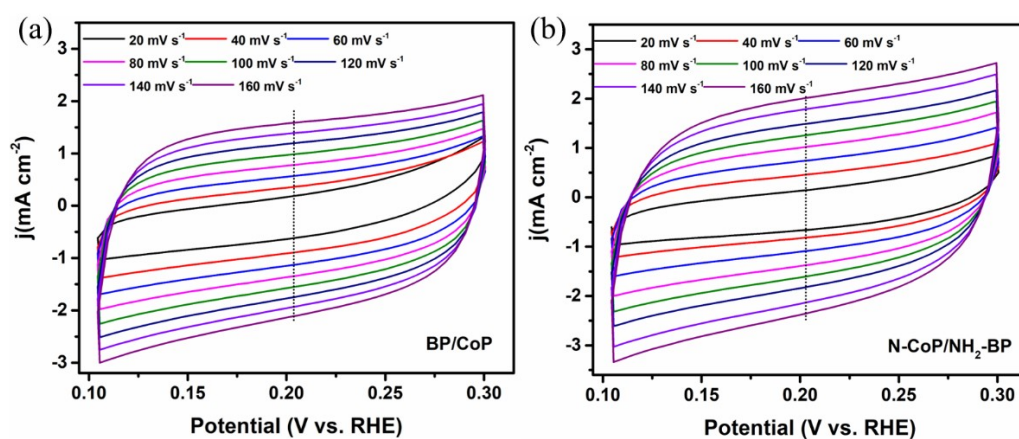


**Figure S7.** CV curves of BP/CoP and N-CoP/NH<sub>2</sub>-BP at different scans.

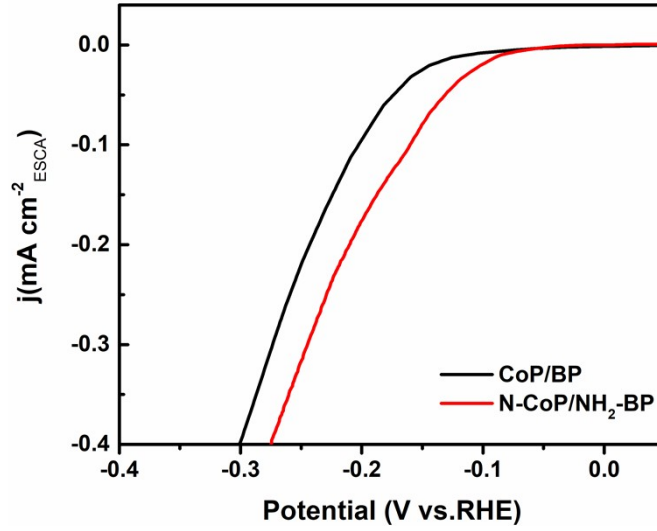


**Figure S8.** Polarization curves with current density normalized by ECSA for N-CoP/NH<sub>2</sub>-BP and CoP/BP.

**Note S1. Turn over frequency (TOF) of N-CoP/NH<sub>2</sub>-BP and CoP/BP catalysts.**

The obtained specific capacitance is converted into the ESCA according to the specific capacitance value of a flat standard material with a real surface area of 1 cm<sup>2</sup>. Literatures reported that the specific capacitance value of a flat surface is usually in the range of 20~60 μF•cm<sup>-2</sup>. In this work, we presume the standard capacitance value of the flat surface as 40 μF•cm<sup>-2</sup> for the following calculations of ESCA.

According to the ESCA calculation equation of the catalyst:

$$ESCA = \frac{C_{dl}}{C_s}$$

Where C<sub>dl</sub> is the double layer capacitance, and C<sub>s</sub> is the standard capacitance value of the flat surface. As a result, the ESCAs of N-CoP/NH<sub>2</sub>-BP and CoP/BP were calculated to be 635 and 517 cm<sup>2</sup>.

The total number of hydrogen turnovers was obtained from the geometric density based on the following formula.

$$n_{H_2} = \left( j \frac{mA}{cm^2} \right) \cdot \left( \frac{1C \cdot S^{-1}}{1000mA} \right) \cdot \left( \frac{1mol e^-}{96485.3C} \right) \cdot \left( \frac{1mol H_2}{2mol e^-} \right) \cdot \left( \frac{6.022 \times 10^{23} H_2 \text{ molecules}}{1 mol H_2} \right)$$

$$= 3.12 \times 10^{15} \frac{H_2/S}{cm^2} per \frac{mA}{cm^2}$$

In the N-CoP/NH<sub>2</sub>-BP and CoP/BP heterostructures, the CoP was homogeneously dispersed on the surface of BP nanosheets. Since the exact hydrogen bonding sites are not clear, we conservatively assume the number of active sites as the total number of surface sites, including both Co and P atoms as possible active sites, from the roughness factor together with the unit cell of CoP.<sup>11-13</sup> The unit cell parameters of orthorhombic CoP are a=5.076 Å, b= 3.277 Å and c= 5.599 Å. Each unit cell contains 4 Co and 4 P atoms. The volume of unit cell is 93.13 Å<sup>3</sup>. According to the atoms and the volume in each unit cell, we can calculate the surface sites per real surface area.

$$n_{CoP}^{surface\ sites} = \left( \frac{8\ atoms\ per\ unit\ cell}{93.13\ \text{\AA}^3\ per\ unit\ cell} \right)^{2/3} = 1.947 \times 10^{15} atoms \cdot cm_{real}^{-2}$$

Finally, plot of current density can be converted into the TOF plot based on the following formula:

$$TOF_{N-CoP/NH_2-BP} = \frac{(3.12 \times 10^{15} \frac{H_2/S}{cm^2} per \frac{mA}{cm^2}) \times |j|}{surface\ sites \times A_{ESCA}} = 0.0025 \times |j|$$

$$TOF_{CoP/BP} = \frac{(3.12 \times 10^{15} \frac{H_2/S}{cm^2} per \frac{mA}{cm^2}) \times |j|}{surface\ sites \times A_{ESCA}} = 0.0031 \times |j|$$

**Table S2.** Fitting results of the EIS curves in Fig.5e using the equivalent circuit.

Sample	Rs (Ω cm <sup>-2</sup> )	Error%	Rct (Ω cm <sup>-2</sup> )	Error%	CPE	n 0<n<1
N-CoP/NH <sub>2</sub> -BP	0.94	1.64	2.31	1.91	2.08E-2	0.41
CoP/BP	0.99	0.91	3.03	1.14	2.07E-2	0.35

The equivalent circuit includes an electrolyte resistance (Rs), a charge transfer resistance (Rct) and a constant phase element (CPE).



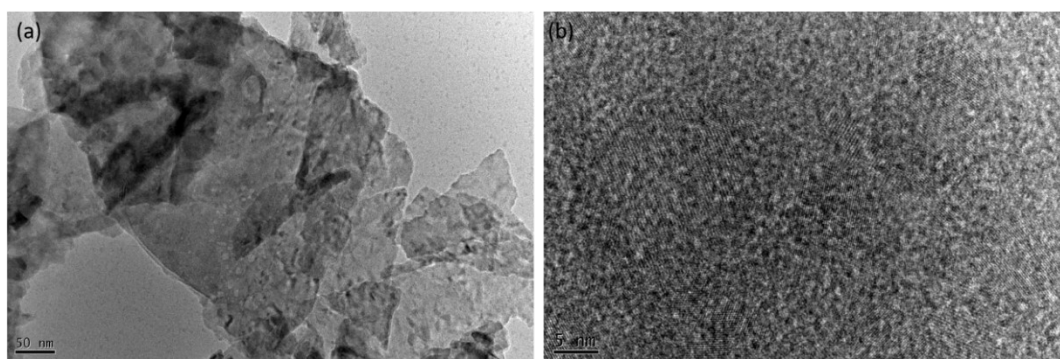


**Figure S9.** HRTEM images of N-CoP/NH<sub>2</sub>-BP after i-t test.

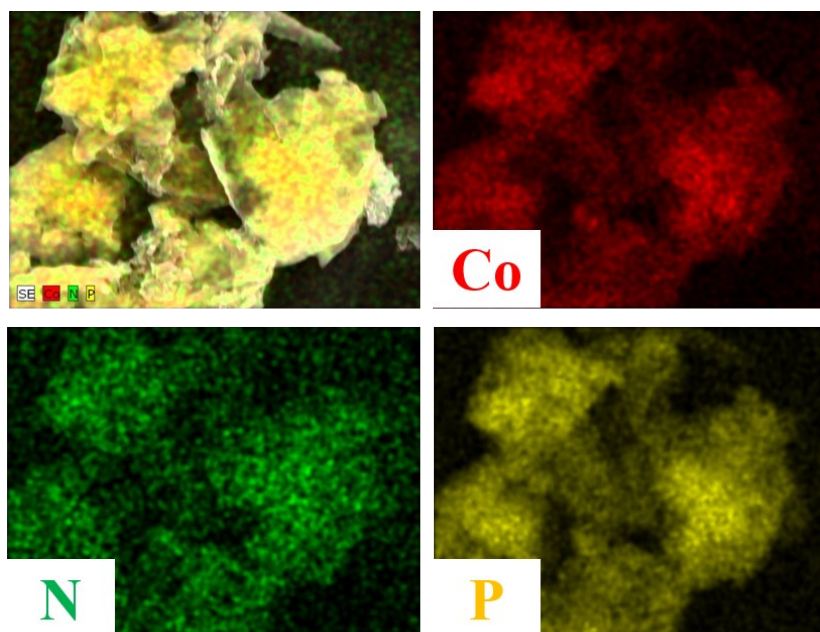


**Figure S10.** The element mapping images of N-CoP/NH<sub>2</sub>-BP after HER test.



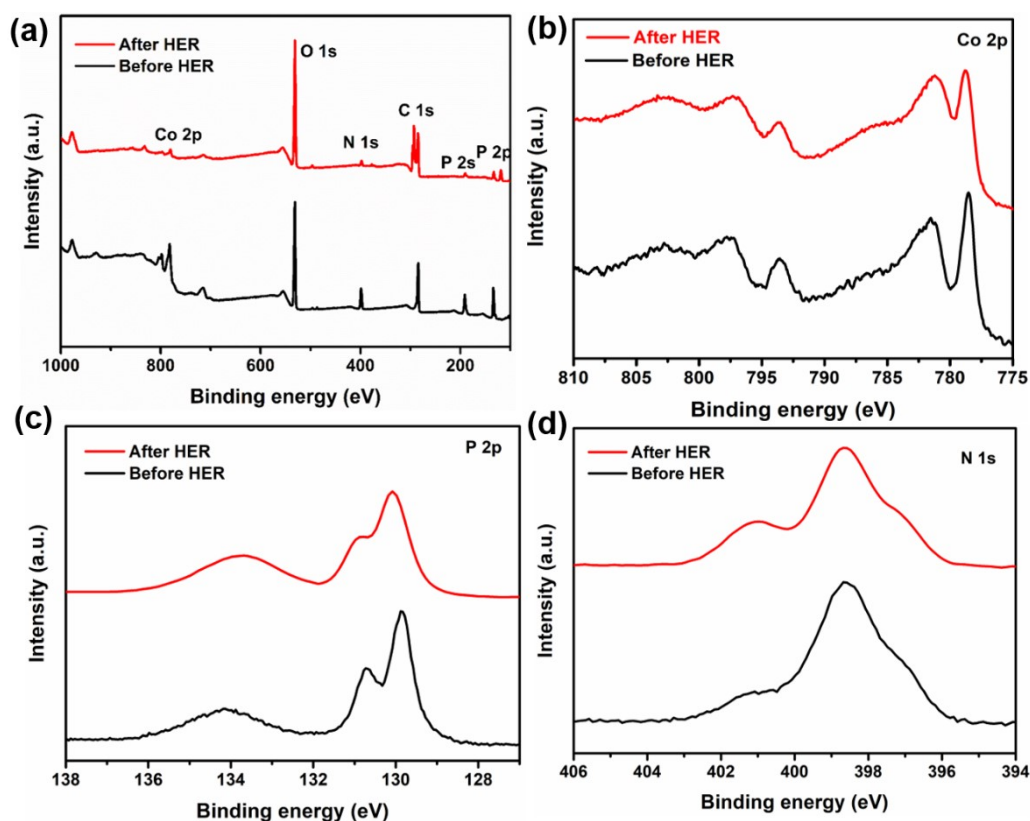


**Figure S11.** (a) XPS survey, high-resolution XPS spectra of (b) Co 2p, (c) P 2p, and (d) N 1s of the N-CoP/NH<sub>2</sub>-BP electrode before and after stability test. The Co 2p, P2p, and N1s spectra were normalized. In Figure S11a, the peak at 119 eV in XPS spectrum after HER is attributed to Al<sub>2s</sub> peak of substrate.

## References

1. X. Wang, L.C. Bai, J. Lu, X. Zhang, D.N. Liu, H.H. Yang, J.H. Wang, P.K. Chu, S. Ramakrishna, X.-F. Yu, *Angew. Chem. Int. Ed.* 2019, 58, 19060-19066.
2. J.H. Wang, D. Liu, H. Huang, N. Yang, B. Yu, M. Wen, X. Wang, P.K. Chu, X.-F. Yu, *Angew. Chem. Int. Ed.* 2018, 57, 2600-2604.
3. X.-D. Zhu, Y. Xie, Y.-T. Liu, *J. Mater. Chem. A* 2018, 6, 21255-21260.
4. L. Shao, H. Sun, L. Miao, X. Chen, M. Han, J. Sun, S. Liu, L. Li, F. Cheng, J. Chen, *J. Mater. Chem. A* 2018, 6 (6), 2494-2499.
5. Y.J. Li, W. Pei, J.T. He, K. Liu, W.H. Qi, X.H. Gao, S. Zhou, H.P. Xie, K. Yin, Y.L. Gao, J. He, J.J. Zhao, J.H. Hu, T.-S. Chan, Z. Li, G.F. Zhang, M. Liu, *ACS Catal.* 2019, 9 (12), 10870-10875.
- (6) R. He, J. Hua, A. Zhang, C.H. Wang, J.Y. Peng, W.J. Chen, J. Zeng, *Nano. Lett.*

2017, 17 (7) 4311-4316.

- (7) Z.-Z. Luo, Y. Zhang, C.H. Zhang, H.T. Tan, Z. Li, A. Abutaha, X.L. Wu, Q.H. Xiong, K.A. Khor, K. Hippalgaonkar, J.W. Xu, H.H. Hng, Q.Y. Yan, *Adv. Energy Mater.* 2016, 7 (2) 1601285.
- (8) C.C. Mayorga-Martinez, N. Mohamad Latiff, A.Y. Eng, Z. Sofer, M. Pumera, *Anal. Chem.* 2016, 88, 10074-10079.
- (9) Q.W. Zhou, Z.H. Shen, C. Zhu, J.C. Li, Z.Y. Ding, P. Wang, F. Pan, Z.Y. Zhang, H.X. Ma, S.Y. Wang, H.G. Zhang, *Adv. Mater.* 2018, 1800140.
- (10) C. Zhang, Y. Huang, Y. Yu, J. Zhang, S. Zhuo, B. Zhang, *Chem. Sci.* 2017, 8 (4), 2769-2775.
- (11) J. Kibsgaard, C. Tsai, K. Chan, J.D. Benck, J.K. Nørskov, F. Abild-Pedersen, T.F. Jaramillo, *Energy Environ. Sci.* 2015, 8, 3022-3029.
- (12) E.J. Popczun, C.G. Read, C.W. Roske, N.S. Lewis, R.E. Schaak, *Angew. Chem. Int. Edit.* 2014, 53 (21), 5427-5430.
- (13) Y.Q. Jing, H.L. Liu, R.J. Yan, J. Chen, H.T. Dai, C.L. Liu, X.D. Zhang, *ACS. Appl. Nano. Mater.* 2019, 2(9), 5922-5930.